Progress in Disaster Science 14 (2022) 100235

Contents lists available at ScienceDirect

Progress in Disaster Science

journal homepage: www.elsevier.com/locate/pdisas

Applying Google earth engine for flood mapping and monitoring in the downstream provinces of Mekong river

Bui Phan Quoc Nghia [a,1], Indrajit Pal [a,1], Nuwong Chollacoop [b,2], Anirban Mukhopadhyay [a,1,*]

[a] Disaster Preparedness, Mitigation and Management, Asian Institute of Technology, Thailand
[b] National Energy Technology Center (ENTEC), National Science and Technology Development Agency (NSTDA), Thailand

ARTICLE INFO

Keywords:
Mekong flood
Flood shifting
Flooding
GEE (Google Earth Engine)
SAR (synthetic aperture radar)

ABSTRACT

Flood is a hazard, but it is also essential for the local communities in the Mekong Delta, as it also provides nutrients for agriculture and resists saltwater intrusion. In recent years, changes in flood patterns have been observed in the Mekong Delta with erratic fluctuations in the flooded area, especially in the downstream provinces. It causes a lot of difficulties in flood monitoring and management in this area. Therefore, a robust assessment of flood shifting is essential in the Mekong Delta. This work addresses the development of a logical model based on Google Earth Engine (GEE) using Sentinel-1 synthetic aperture radar (SAR) data to assess floods in the downstream Mekong River basin. In the present study, the observed data of Tan Chau and Chau Doc hydrological stations have been used to test and prove the reliability of this application. The inundation scenario generated from this study showed a gradual shift in flooding patterns of the downstream provinces of the Mekong Delta. Overall, the flooded area is decreasing; however, the same is increasing in Bac Lieu province. This research will help to construct a professional support system to monitor the flood inundation in the Mekong Delta. They can give local authorities a big picture of inundation to decide on flood disaster preparedness, mitigation, and adaptation.

1. Background

The Mekong Delta of Vietnam (MDV) is the third-largest delta in the world, located in the downstream area of the Mekong River before the river drains into the East Sea of Vietnam [23]. According to General Statistics Office (GSO), the total area of MDV is approximately 04 million ha, with a total population of more than 17 million [13]. This area leads the rice and aquaculture production of the nation, and the economic growth rate of the MDV is higher (7.8%) than the national average (6.8%) [13]. Historically, the MDV had a favourable climate condition and a low rate of natural disasters compared to other regions of Vietnam; however, this area has been faced many severe hazards such as water scarcity, drought, saltwater intrusion, and coastal erosion in recent years [23,30,42,43].

Based on the country report of the ASEAN Coordinating Centre for Humanitarian Assistance on disaster management (AHA Centre), the MDV is a hot spot for flood and inundation in Vietnam [2]. Flood brings benefits as well as damages and losses. Extreme floods can cause human loss, and destruction of infrastructure and agriculture. However, seasonal floods have played an essential role in providing aquatic resources, freshwater, and nutrients [30,44,45]. The regular flooding season in the study area is between June and the end of November [21], with high-intensity flooding in September and October. The MDV is inundated almost every year, ranging from 1.4 million hectares during small floods to 1.9 million hectares during big floods [44]. Based on the analysis of water levels from 1990 to 2019, Le [21] found that the trend of the big flood is decreasing, and small flood is increasing. However, flood is impacted by tides and surges in the coastal provinces more than upstream river discharge [41].

Flood hazard pattern has been observed to be shifted in the MDV with the erratic fluctuations of the flooded area in the downstream provinces and the increasing flooding trend in urban areas because of the development of irrigation systems, sea level rise, high tides, and subsidence (T. A. [21,41,45]). For example, based on observed data, the

* Corresponding author.
E-mail addresses: bpqnghia@gmail.com (B.P.Q. Nghia), indrajit-pal@ait.ac.th (I. Pal), nuwong.cho@entec.or.th (N. Chollacoop), anirban@ait.asia (A. Mukhopadhyay).
[1] Disaster Preparedness, Mitigation and Management, Asian Institute of Technology, Thailand, Pathumthani,12,120
[2] The National Energy Technology Center, National Energy Technology Center, Thailand, Pathumthani,12,120

https://doi.org/10.1016/j.pdisas.2022.100235
Received 23 March 2022; Received in revised form 16 May 2022; Accepted 20 May 2022
Available online 24 May 2022
2590-0617/© 2022 The Authors. Published by Elsevier Ltd. This is an open access article under the CC BY-NC-ND license (http://creativecommons.org/licenses/by-nc-nd/4.0/).

water level at Can Tho station – a downstream station in MDV – was 2.15 m in 2011, higher than that of 2000 (1.79 m). Meanwhile, the water level of Tan Chau – an upstream station in MDV – was 4.27 m in 2011, lower than 4.90 m in 2000 [9]. The shift of flooding areas may impact policymakers' decisions in many aspects such as water management, land use, urban management, etc. Therefore, monitoring flooding areas and the shift of flood patterns is vital for understanding the concurrent situation of flood and helps decision-makers give appropriate solutions promptly.

Synthetic aperture radar (SAR), a type of space-based sensor, has proven its ability to monitor and map flood extent [3,17]. SAR is beneficial compared to other sensors since its radar transmission in the microwave spectrum is unaffected by cloud, heavy rain, and visibility [39,40]. Flood hazard mappings derived from SAR data could be vital evidence for efficient disaster risk management enabling social relief groups and key stakeholders to gather spatially accurate intelligence on flood events in a prompt and cost-effective approach [49]. Floods are emerging as a grave issue in our changing climate. Flood mapping is crucial for both risk assessment and forecast improvement. Since SAR data is adequate for flood risk assessment, many flood mapping methods have been devised in recent years [35,46]. conducted a study using Sentinel-1-SAR-based flood assessment by incorporating daily and monthly rainfall data obtained from the IMD ("Indian Meteorological Department") and TRMM ("Tropical Rainfall Measuring Mission") for delineating the regions swamped by floodwaters across Kerala, India, during the monsoon season of 2018. Landuyt et al. [20] reviewed and assessed different flood mapping approaches, including enhanced thresholds, contour modelling, and change detection, while evaluating the strategies using intermediate resolution SAR data from various flooding events in the UK and Ireland. Long et al. [24] used SAR data and a novel flood estimation approach termed CDAT ("Change Detection and Thresholding") to outline the flood extent of Namibia's Chobe floodplain. Pulvirenti et al. [51] utilized SAR data to map submerged zones using fuzzy logic. It is planned to integrate this tool into the Italian Public Security's operation flood management structure and to test it on a recent flooding event in Albania.

Google Earth Engine (GEE) is introduced as the world's most advanced cloud-based geospatial processing platform that can overcome processing problems encountered by traditional satellite image processing methods [12,40]. GEE provides a cloud computing platform to store and analyse huge data sets up to petabytes in size for ultimate decision making and analysis [18]. Google has incorporated the Landsat data sets into its cloud computing platform since the series became freely available in 2008 [28]. On a regional and global scale, researchers have utilized the GEE to investigate the dynamics of land regions such as forest/ vegetation cover [14,16], surface waterways [8,33,38], and human habitation [8]. It has been employed to assess current agrarian diversification [29,31,50] and for other purposes. The GEE maintains a huge geospatial data repository, including Sentinel-1 GRD ("Ground Range Detected") data that is constantly updated [6]. Due to the intricacy of SAR preprocessing, analysis-ready SAR datasets available on GEE represent a huge step forward for application-based remote sensing through SAR. GEE's dataset comprises over 40 years of archival earth observation imageries regularly updated in quantity and quality, including SAR data [12].

This study aims to assess the flood shifting pattern in the MDV by utilising GEE (Google Earth Engine) and Sentinel-1 SAR (synthetic aperture radar) data products to visualise flooded areas in the MDV. The flood maps were cross-checked with available datasets and observation stations. Then the flooded areas were correlated with water levels and different provinces. The correlation could be served as a baseline report for much-talked flood shifting in the downstream Mekong River. Moreover, the coherence of the flooded area and the water level of the upstream stations are examined annually. Finally, the shift in flooding area per province has been detected, along with the quantification of the relationships established. This study will help the policymakers, and concerned authorities mitigate flood hazards, water security, and construction planning.

2. Study area, data, and methodology

2.1. Study area and data

The study area was the MDV's eastern coastal provinces: Tien Giang, Ben Tre, Tra Vinh, Soc Trang, Bac Lieu, and Ca Mau. The flooding area in these provinces is usually less than in other upstream provinces. The locations and boundaries of the study area, MDV, An Giang province, and Tan Chau and Chau Doc stations are shown in Fig. 1.

The Mekong River is the longest (4800 km) in Southeast Asia, with a drainage basin of approximately 7.95×105 km^2 area (T. V. H. [22]). The Mekong River Delta (MRD) encompasses a 4.95×104 km^2 area, of which 74% falls in Vietnam. The MRD in Vietnam could be characterized by a vast floodplain with numerous rivers and channels, creating a complex network. The MRD experiences dual tidal activity, one from the South China Sea and the other from the Gulf of Thailand. Climatic conditions follow a typical monsoonal pattern with two distinct seasons. The rainy season starts in May and ends in October, and the dry season starts in November and ends in April. Numerous canals across the delta in Vietnam were constructed for various purposes, and dykes, and weirs were made to fight against floods and associated hazards. These constructions disrupt the seasonal variability of the freshwater flow of the Mekong River [34].

Three different types of data have been used in this study (Table 1). Firstly, the Sentinel-1 SAR Vertically transmitted Vertically receives (VV) polarization data. VV is used instead of vertically transmitted Horizontally received (VH) because it is more efficient in flood mapping [1,5,46]. Secondly, the administrative boundaries of the whole study area and each province were downloaded from the Human Data Exchange and updated in 2020. Finally, the Mekong River Commission data have been collected for the highest water level data at Tan Chau and Chau Doc hydrometeorological stations during the flood season from June to December from 2015 to 2020. Tan Chau and Chau Doc hydrometeorological stations are two upstream stations of the Tien and Hau rivers. They are located in An Giang province. The amount of water discharged through these two rivers covers 80 to 85% of the amount of water in the MDV (T. A. [21]).

2.2. Methodology

The methodology is divided into two figures; Fig. 2 describes the methods adopted for flood area calculation using GEE, and Fig. 3 depicts the statistical operations performed to analyse the results.

Fig. 3 depicts the general approach of this work, which depicts the logical model built up to assess the reliability of the flooded area given by GEE and Sentinel-1 SAR data, and then detects changes in flooding patterns across the study area and each province. It can be divided into three main processes as follows: The first process is to check the flooded area's reliability generated by the GEE database of Sentinel-1 SAR imageries. Two factors further prove the reliability. First, from June to October of each year, a correlation was performed between the flooded area of An Giang province from GEE and observed data of the highest water level in Tan Chau and Chau Doc stations. This study uses the coefficient of determination (R^2) to determine the correlation between flooding areas from GEE and water level. In addition, *P*-value shows the statistically significant difference between flooding areas from GEE and water level. If the results are good with $R^2 \geq 0.7$ and p-value <0.05, the reliability is high [10,36]. If not, the code of flood calculation needs to be revised. The reason for choosing 02 stations Tan Chau and Chau Doc to evaluate the correlation is 2.1. These stations are 02 upstream stations of Tien River and Hau River, through which the amount of water discharge covers from 80 to 85% of the amount of water in the MDV.

Secondly, this study comprises the coherence of the flooding area of

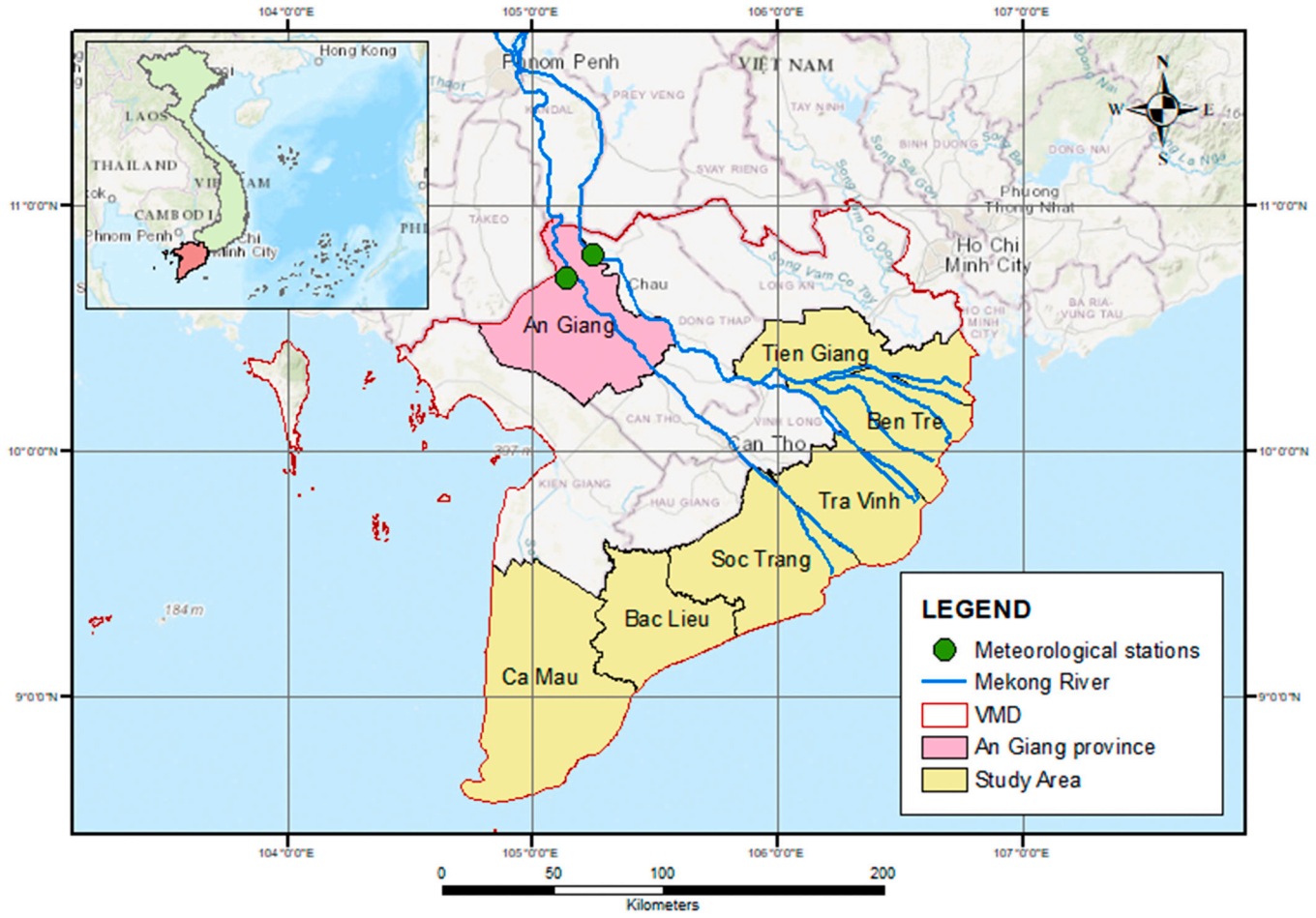

Fig. 1. Map of the study area (06 East coastal provinces of the MDV).

Table 1
Data specification.

No.	Data	Description	Sources
1	Sentinel-1 SAR	- Polarization: VV polarization 1 - Bands: 1 - Wavelength: 5.5 - Spatial resolution: 20 m × 20 m - Swath: 250 - Temporal resolution: 12 days	Google Earth Engine: https://developers.google.com - Acquisition date: 29 October 2021
2	Shapefile of the study area	Administrative boundary of MDV, An Giang province, study area	The Humanitarian Data Exchange https://data.humdata.org/ - Acquisition date: 29 October 2021
3	Highest water level	- Station: Tan Chau (10°48' 105°13'), Chau Doc (10°42' 105°06') in An Giang province - Temporal resolution: Highest water level from June to October each year from 2017 to 2020 in Tan Chau and Chau Doc station	Mekong River Commission for sustainable development http://ffw.mrcmekong.org/ - Acquisition date: 29 October 2021

the MDV and yearly local reports about floods and drought. In addition, the coherence of distribution of flood area and MDV terrain is also considered. The process entails detecting changes in flood patterns in the study area and each province. In terms of flooded areas, the R^2 value is used to estimate the correlation between MDV and the total study area and between the total study area and each province. R^2 value from 0.7 to 1.0 is strong, from 0.4 to less than 0.7 is medium, and from 0.0 to less than 0.4 is weak [36]. Similarly, *P*-values have been applied to show the statistically significant difference between the MDV and the study region and between each province's studied area. The threshold is 0.05 [10]. P-value less than or equal to 0.05 proves no significant flood shifting; on the other hand, greater than 0.05 means significant flood shifting. Because the study area is within MDV, and each Eastern coastal province is within the study area, if the flooding area in the MDV increases, the flooding area inside the study area and each province will increase and vice-versa (Fig. 4).

The last part is to conclude flood pattern shifting in the study area. Local reports about flood shifting and hazards are reviewed to understand the reliability and relevance of the results of flood shifting from GEE and Sentinel-1 SAR images.

The most important part of the methodology is decoding Sentinel-1 SAR data to identify the flooded areas. This section involves deploying the JavaScript programming language directly implemented on the GEE interface (https://developers.google.com/earth-engine). In this study, the code is developed based on the UN online course about flood mapping using Sentinel-1 SAR data in GEE (https://t.ly/0FdC). It includes command declaration tasks to import image data to the platform, image processing, image analysis, result visualisation, and result exporting. In this study, pixel values of pre-flood and post-flood scenario images have been compared. This difference helps to separate pixels that belong to the permanent water bodies such as rivers and wetlands and pixels that represent waterlogged areas during the flooding season.

Flood mapping and inundated area calculation methodology are as follows:

The Sentinel-1 data package and study area boundary have been

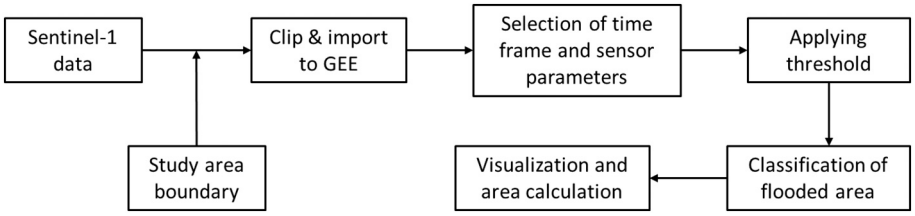

Fig. 2. Processing of Sentinel-1 SAR data using GEE platform.

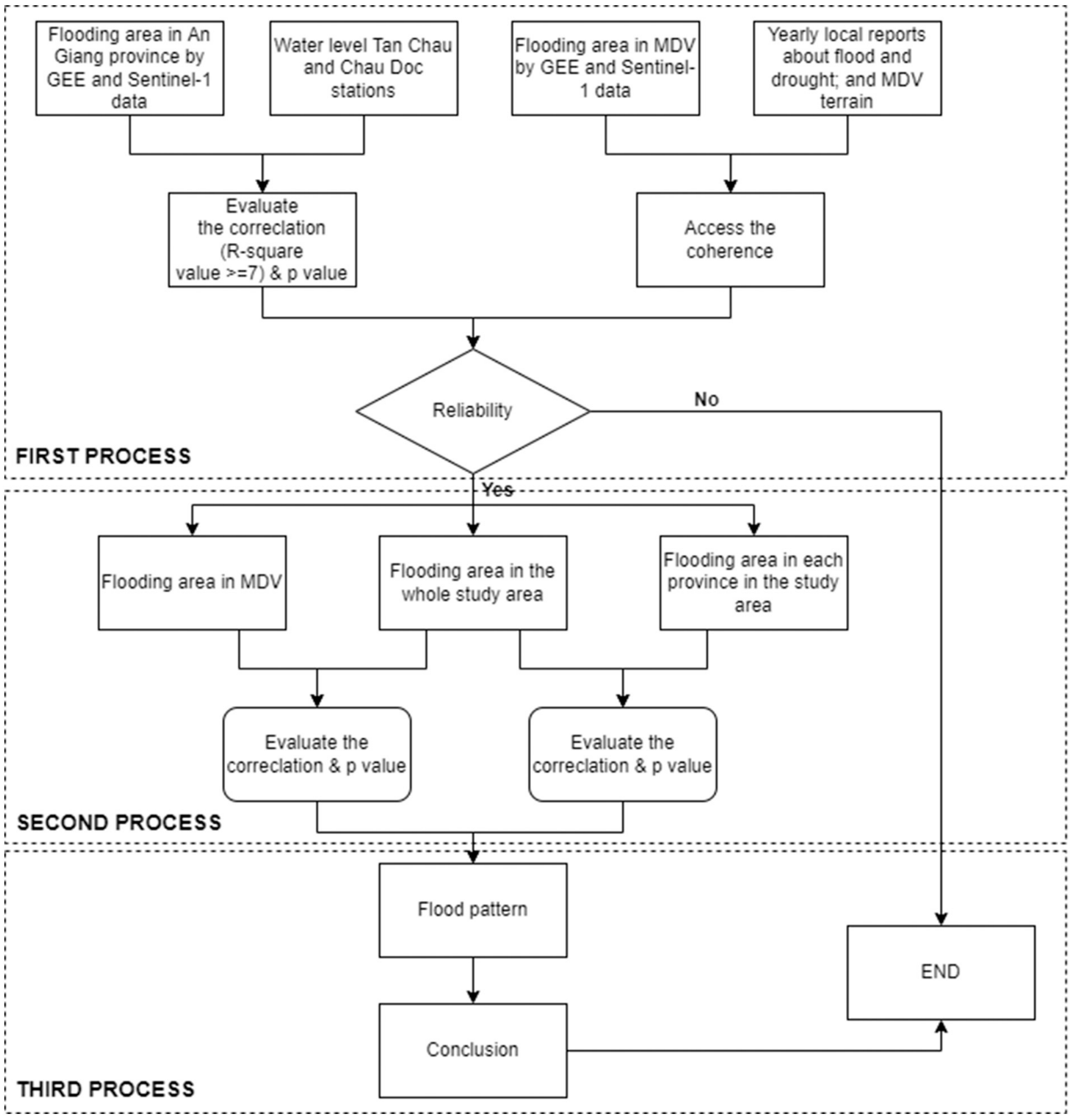

Fig. 3. Schematic representation of the statistical operations performed in this study.

imported to GEE in the first step. The boundaries are designated as the shapefiles of the MDV on a province level. They were directly imported into the Assets of GEE. In the next step, Time frame and sensor parameters were specified for this study. The base period selected for flooding area comparison is 1st to 31st May of each year (right before the start of the flood season). The pre and post-flood period are 1 June and 30st November of each year because flood usually starts in June and ends in November every year (T. A. [21]). By setting periods, not single dates, the selection can cover enough tiles of the selected area. Sensor parameters specified are polarization "VV" and a "descending" pass direction. The difference threshold was "1.25" because this value is usually used for GEE flood detection [19,37]. The flood extent was

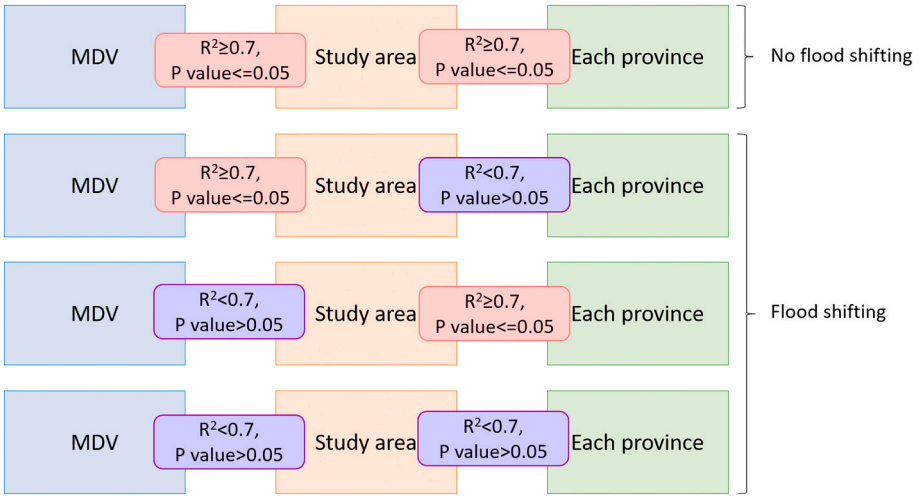

Fig. 4. All cases of correlation of flood area between MDV, study area and each province.

determined when the pixels representing the flooded area were classified correctly. The primary comparison is the difference between the before and after imageries. After applying the predefined threshold, the flood extent mask is created, and the flood result is refined. Each year, the flood extent area is calculated. Finally, the flooded area was approximated by summing all the pixels representing the flooded regions and translating the flood extent to hectares. Finally, the inundated area was visualised by importing the geographic information system application results. The result of the flood extent area has been acquired from GEE and visualised in QGIS. It is a cross-platform desktop geographic information system (GIS) tool to browse, edit, and analyse geographical data without payment.

3. Results

3.1. The coherence of flooding area from GEE and observed data

The coherence of the flooding area from GEE and observed data is

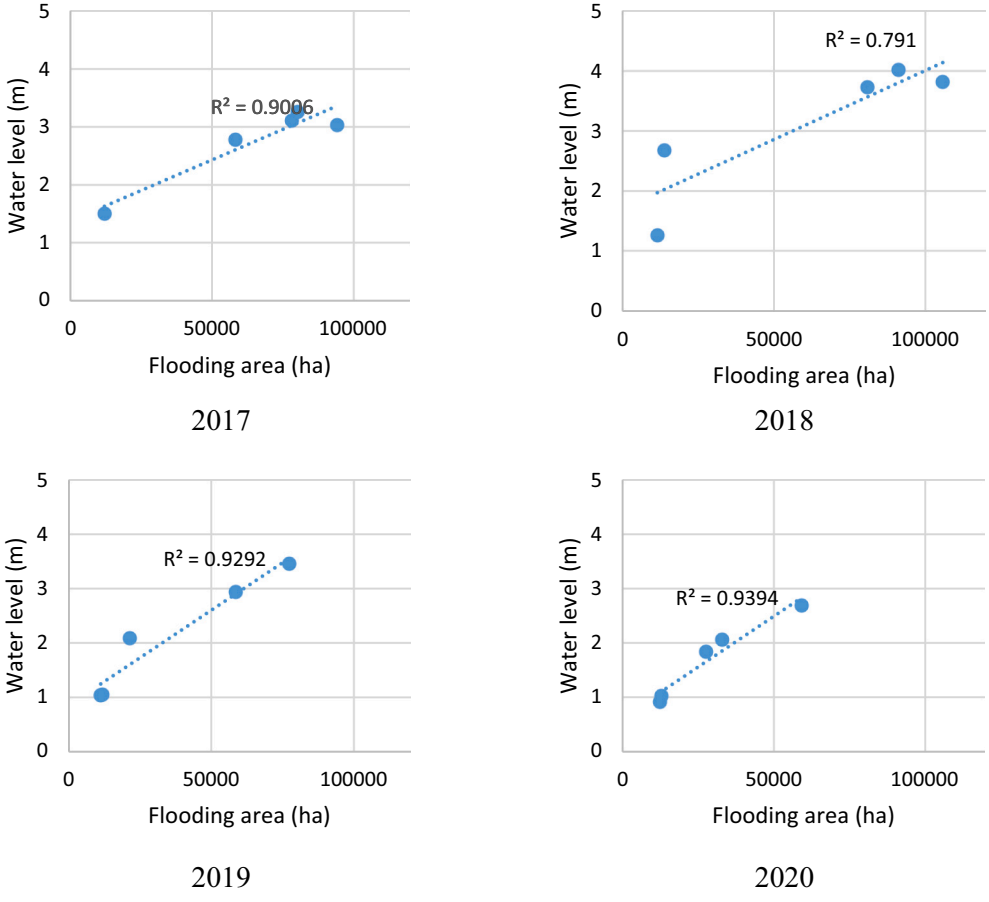

Fig. 5. Correlation between flooding area in An Giang province and water level in Tan Chau station in June to October from 2017 to 2020.

proved by the correlation and the *p*-value between the flooding area in An Giang province and the water level in Tan Chau and Chau Doc stations of An Giang province from June to October 2017 to 2020. Fig. 5 shows the correlation between Tan Chau station's water level and the flooding area in the Giang province. R2 ranges from 0.791 to 0.9394 from 2017 to 2020. R2 in 2018 is the lowest, with 0.791. In other years, the R2 value is higher than 0.90.

Fig. 6 describes the coherence of the water level in Chau Doc station and the flooding area in An Giang province. The R^2 value is between 0.8144 and 0.9497. The year 2016 is the lowest with 0.8144, and 2020 is the highest with 0.9497. These graphs also show the linkage between water level and flooding area. When the water level increases, the flooding area will increase and vice versa. Table 2 describes the *p*-value of the flooded area in An Giang province and the water level in Tan Chau and Chau Doc stations from June to October from 2017 to 2020. The highest one is 0.043423, which is still below the threshold of 0.05.

Another indicator of the code's dependability is the coherence between flooding areas in MDV and weather changes from 2015 to 2020. The flooding area of the whole MDV from 2015 to 2020 is demonstrated in Fig. 7 and visualised in Fig. 8. In Fig. 7, it can be seen that the periods from 2015 to 2016 and 2019 to 2020 have low flooded areas, while the period from 2017 to 2018 represents high flood incidents. Because there were severe droughts in the dry season during 2015 /2016 and 2019 /2020, which was reported in the Global Facility for Disaster Reduction and Recovery (GFDRR) and Ministry of Agriculture and Rural Development (MARD) [11,25]. The negative trend in flooded areas is also coherent with recent research about the long-term decrease of water discharge to the MDV because of climate change, riverbed mining and upstream dams [15,30,47]. Fig. 8 also shows the flood area distribution, and it is close to reality. The upstream area is covered with floods more than the downstream and coastal areas. Only one part of the upstream area that is not flooded during flood season is the Bay Nui mountainous area of An Giang province, the highest elevated area in the MDV, with a

Table 2
The *P*-value of flooding area in An Giang province and water level in Tan Chau and Chau Doc stations from June to October from 2017 to 2020.

		Flooding area in An Giang province			
		2017	2018	2019	2020
Water level	Tan Chau station	0.013715	0.043423	0.008168	0.006443
	Chau Doc station	0.036041	0.016001	0.006453	0.004858

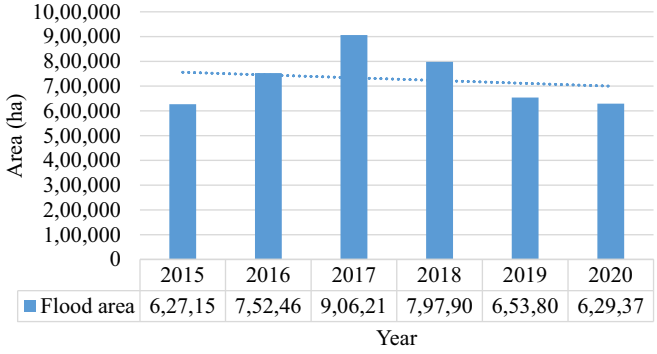

Fig. 7. Flooded area of the MDV over the years.

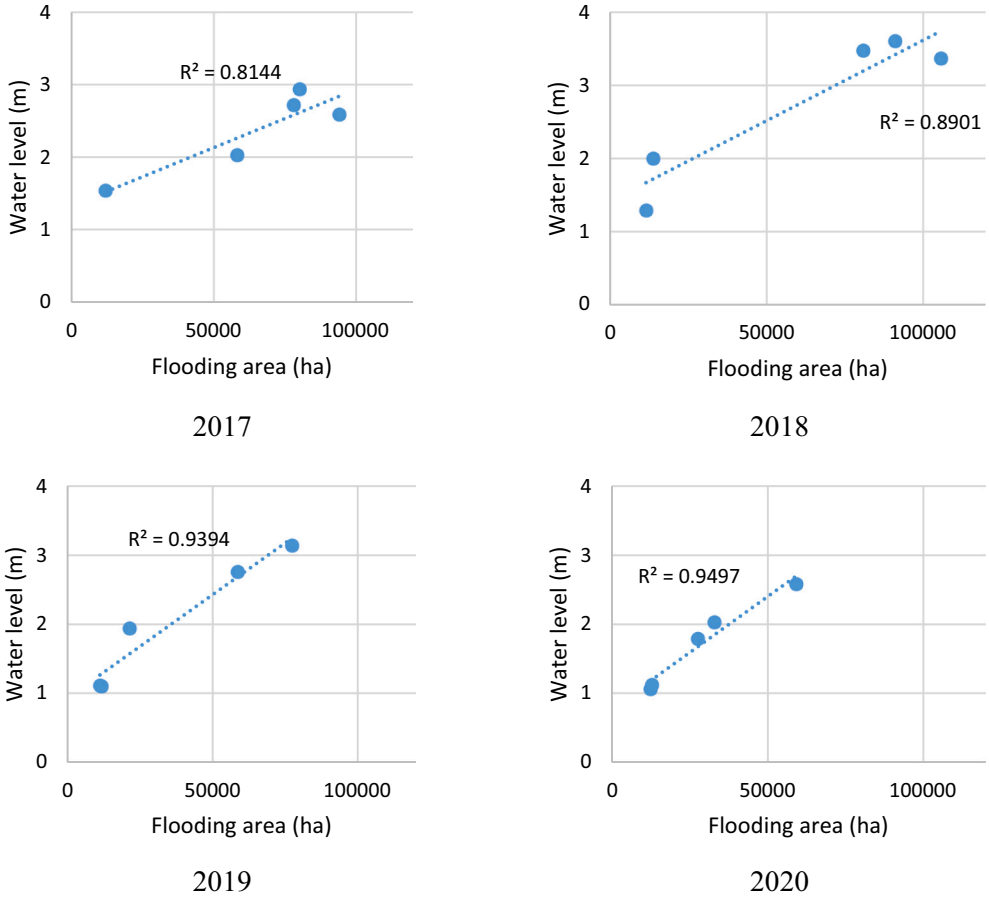

Fig. 6. Correlation between flooding area in An Giang province and water level in Chau Doc station in June to October from 2017 to 2020.

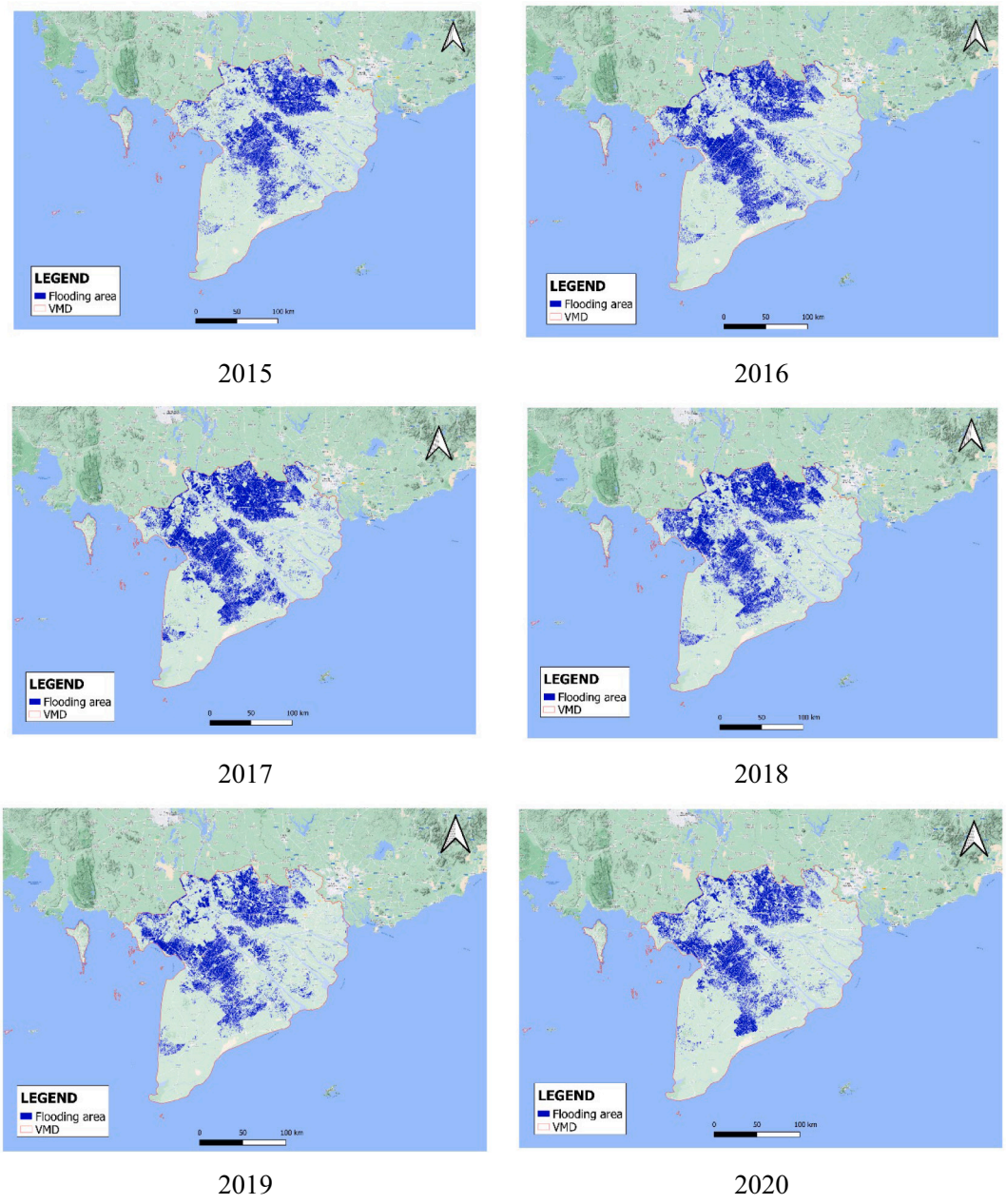

Fig. 8. Spatial representation of flooding area of the MDV.

peak of 705 m [4].

The correlation and the *p*-value between the flooded area in An Giang province and the water level in the chosen stations; and the consistency between the flooded area in MDV and local reports about disasters and topology show that the code in this study is reliable. These results also support the findings of Vanama et al. [48], Moothedan et al. [27], and Moharrami et al. [26] that the resultant flood area and maps from GEE have high accuracies, and it proves that GEE is an efficient way for rapid flood mapping.

3.2. The shift of flooding area of the eastern coastal provinces from 2015 to 2020

Fig. 9a shows the flood area of the study area and its trend from 2015 to 2020. It can be observed that the trend decreases slightly, the same as the trend of the MDV. According to GSO, the total area of 06 coastal provinces is 1846.6 thousand ha accounting for about 45.2% of the total area of the MDV [13]; however, the total flooding area is only from 15% to 20% of the total flooding area of Mekong Delta. It is understandable because the study area is downstream of the MDV. A correlation between the flooded area of the study area and the MDV from 2015 to 2020 is shown in Fig. 9b; the p-value is 0.008498, which is less than 0.05; therefore, the flooded area of the study area and the MDV is coherent.

The correlation between the flooded area of MDV and the study area is high, but it is not strong between each province and the whole study area. Fig. 10 describes the correlation of the flooding area between the study area and each province in it. It can be recognized that the R^2 value of Soc Trang province is 0.9634, which is high; the R^2 value of Ca Mau is 0.4758, which is medium; and the R^2 values of Tien Giang, Ben Tre, Tra Vinh, and Bac Lieu are 0.1338, 0.0302, 0.1331, and 0.148 respectively which are in low range. Table 3 describes the p-value of the flooding area between the study area and each province from 2015 to 2020. The p-value in Soc Trang is 0.000508, which is the only one below 0.05; the others are above. They prove that the correlation between the flooding

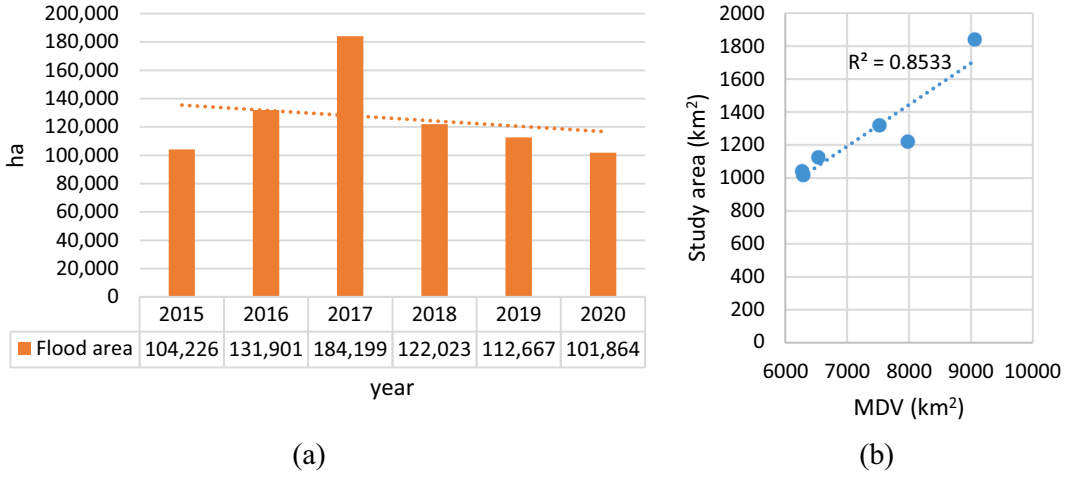

Fig. 9. Flooding area of the study area (a), and correlation of the flooding area between the MDV and study area from 2015 to 2020 (b).

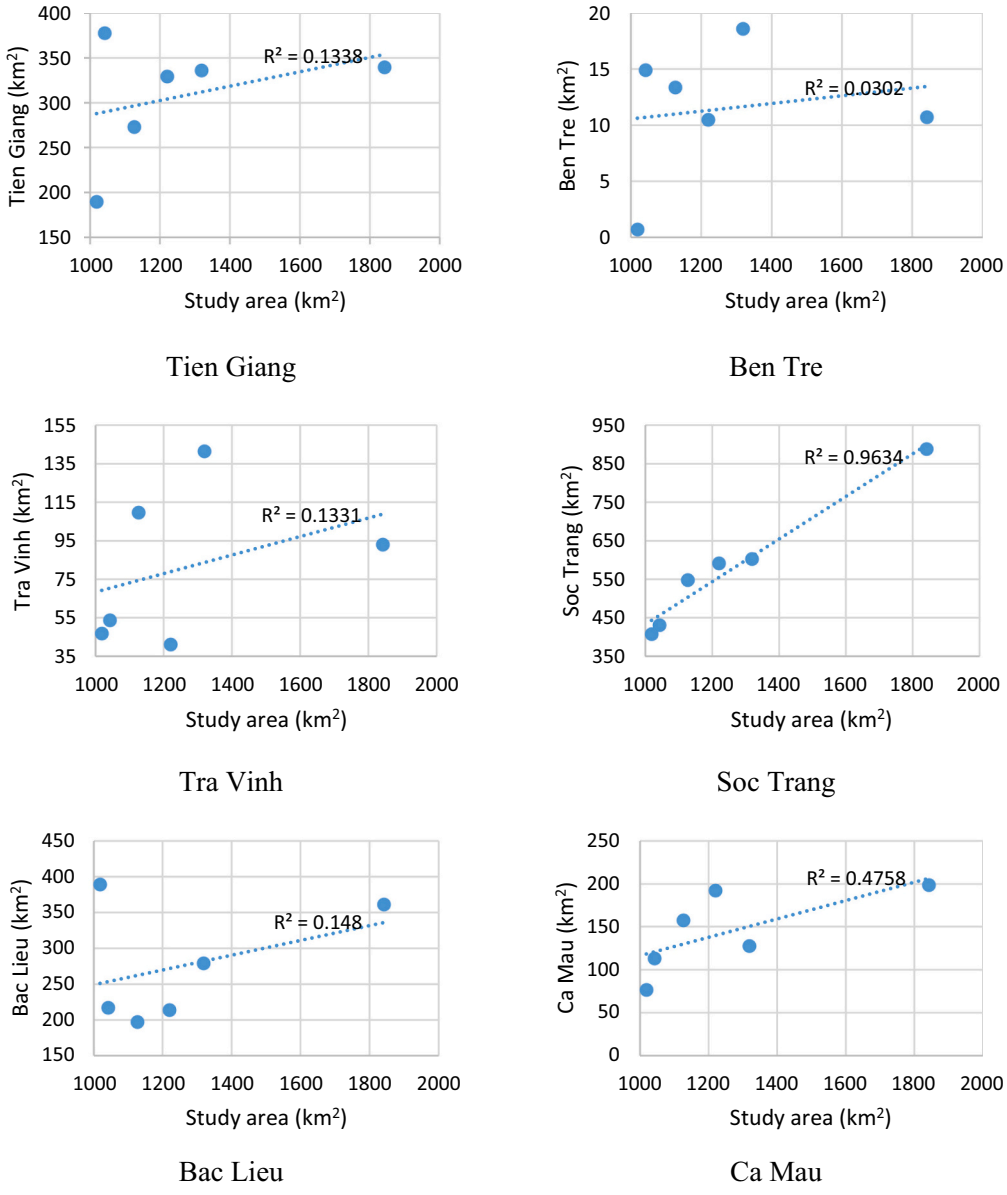

Fig. 10. The correlation of the flooding area between the study area and each province from 2015 to 2020.

Table 3
P-value of the flooding area between the study area and each province from 2015 to 2020.

	Flooded areas in each province					
	Tien Giang	Ben Tre	Tra Vinh	Soc Trang	Bac Lieu	Ca Mau
Flooding area in study area	0.475762	0.741978	0.476956	0.000508	0.451452	0.129423

area, the study area and Tien Giang, Ben Tre, Tra Vinh, and Bac Lieu is low. Therefore, the shift in the flooded area of these 04 provinces is high.

In Fig. 11, it can be observed that the decreasing trend is the same as the trend of the MDV and study area in five provinces, Tien Giang, Ben Tre, Tra Vinh, Soc Trang, and Ca Mau. These negative trends can be the same as the negative trend of water discharge to the MDV: upstream dam building, riverbed mining, and climate change impacts mentioned in part 3.1. However, the decrease is not the same within these five provinces. While Soc Trang, Ca Mau, and Tra Vinh have a slightly decreasing trend, the trend in Tien Giang and Ben Tre decreases dramatically. An increasing trend was observed in Bac Lieu province, which is different from other provinces in the study area and MDV. Especially in 2020, the flooding area in Bac Lieu province is highest. This result is very consistent with the report of the People's Committee of Bac Lieu Province (PCBL) in 2020. The report mentioned a huge flood event in Bac Lieu province in the rainy season. It damaged 18,625.734 ha of agricultural products, including rice, vegetables, and fruit trees [32]. Massive flooding has been mentioned in the report are with high precipitation, tidal peaks, and impacts of storms [32].

According to the results above, it can be concluded that flood shifting is happening in the Eastern coastal area of the MDV. This conclusion is in some way consistent with the study of [30], Dieu and Thao [7], and Triet et al. [45]. This study argued that the flood regime is changing in the MDV due to urbanisation, climate change, sand mining, and irrigation infrastructure building.

4. Conclusion

This study attempts to determine the dynamics in flood patterns of six East coastal provinces downstream of the MDV. Using GEE and its

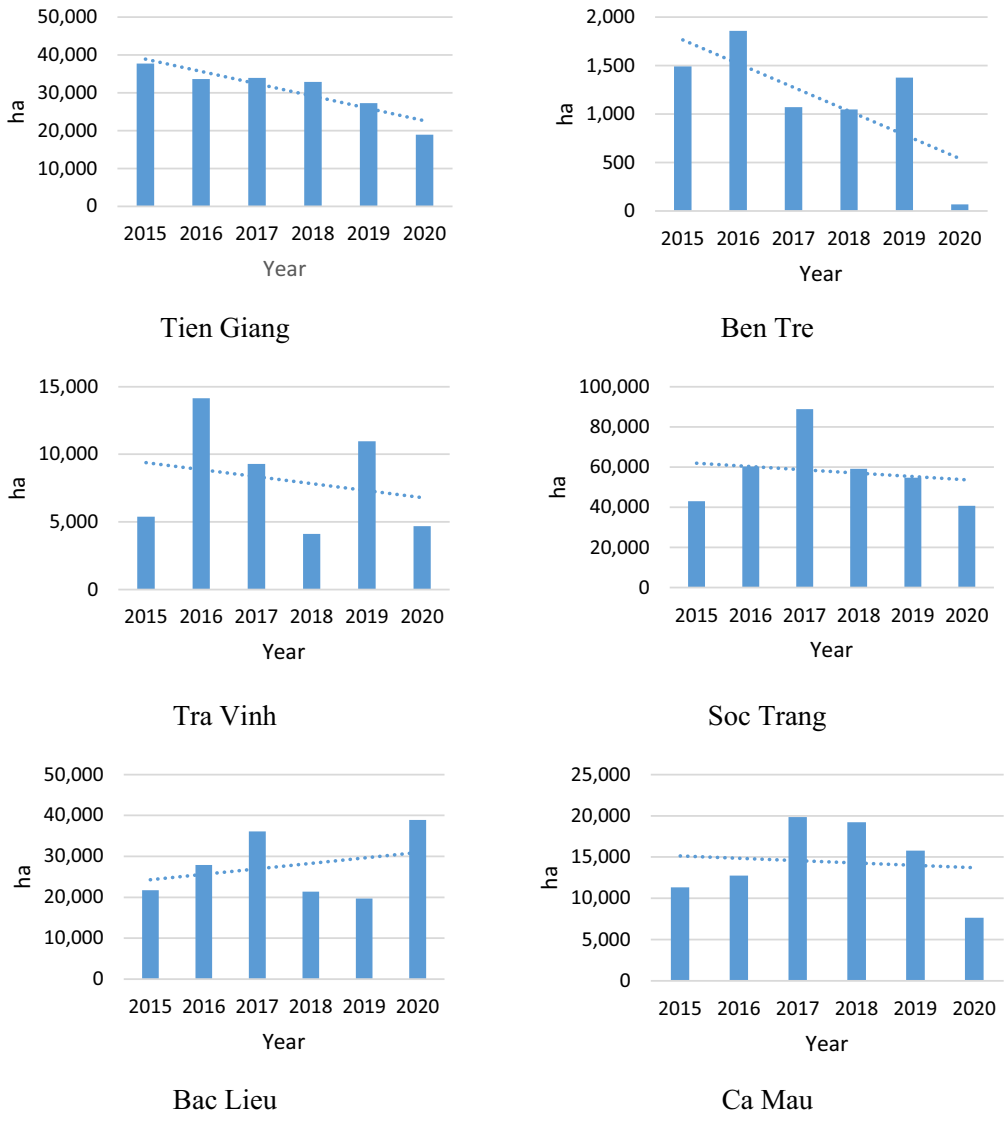

Fig. 11. The trend of flooding area of the 06 East coastal provinces from 2015 to 2020.

Sentinel-1 SAR data database, the model has developed a logic-based approach to map and monitor flooding downstream of the MDV and recognize the correlation between regions regarding flooding. It also compares the results from coding to the observed data and available local government reports, checking the results' reliability.

The study proves that GEE is an admirable platform to monitor and map the flooding across the study area; therefore, it can also monitor the flood in other areas. It is beneficial not only for scientists but also for the local governments, decision-makers, or other persons interested in doing research following flood progression. The result shows that the flood pattern of the whole six east coastal provinces is consistent with the flood pattern of the MDV. However, the dynamics of the flooded area within six East coastal provinces is high. There is potentially a shift in flooding areas within provinces in the study area and the MDV. However, to conclude the shift in flooding areas in MDV, more profound research is needed.

There are many ways to develop more profound research by fields, areas, and methods based on this research. Disaster management, water management, and urban planning are promising fields that can use the result of this research. Each province can rely on this to adapt suitable socio-economic development plans for its own. Some methods, such as combining with observed data or other satellite data, can apply by using the direction of this thesis to compare and give better results for flood mapping and monitoring.

This study has some shortcomings in the result. Firstly, the result is based on the outcome of Sentinel-1 SAR images analysis; therefore, there might be some bias compared to the result from observed data. However, it is still good to quickly track the flood in case of insufficient observed data. Secondly, Sentinel-1 SAR data is only available from 3 October 2014 to the present; thus, this method cannot be used to find the flood progression before 2014.

CRediT authorship contribution statement

Bui Phan Quoc Nghia: Conceptualization, Methodology, Formal analysis, Writing – original draft. **Indrajit Pal:** Conceptualization, Methodology, Writing – review & editing. **Nuwong Chollacoop:** Conceptualization, Methodology. **Anirban Mukhopadhyay:** Methodology, Writing – review & editing.

Declaration of Competing Interest

The authors declare that they have no known competing financial interests or personal relationships that could have appeared to influence the work reported in this paper.

Acknowledgements

The first author of this study, Mr. Bui Phan Quoc Nghia, has received financial support from the Education and Research Collaboration between the National Science and Technology Development Agency (NSTDA) and the Asian Institute of Technology (AIT). The authors would like to thank the Mekong River Commission for sustainable development, ESA, Google Earth Engine, and The Humanitarian Data Exchange for the data used in this study.

References

[1] Agnihotri AK, Ohri A, Gaur S, Das N, Mishra S. Flood inundation mapping and monitoring using SAR data and its impact on Ramganga River in ganga basin. Environ Monit Assess 2019;191(12):1–16.
[2] AHA Centre. Country report Vietnam. *Natural disaster risk assessment and area business continuity plan formulation for industrial agglomerated areas in the ASEAN region*. Jpn Int Cooperat Agency 2015:10–2.
[3] Amitrano D, Di Martino G, Iodice A, Riccio D, Ruello G. Unsupervised rapid flood mapping using Sentinel-1 GRD SAR images. IEEE Trans Geosci Remote Sens 2018;56(6):3290–9.
[4] Canh DN, Thi NTA. Developing Khmer community based rural tourism in Tinh Bien district, an Giang province. Can Tho Univ J Sci 2018;54(6):148–57. https://doi.org/10.22144/ctu.jvn.2018.107.
[5] Carreño Conde F, De Mata Muñoz M. Flood monitoring based on the study of Sentinel-1 SAR images: the Ebro River case study. Water 2019;11(12):2454.
[6] DeVries B, Huang C, Armston J, Huang W, Jones JW, Lang MW. Rapid and robust monitoring of flood events using Sentinel-1 and Landsat data on the Google earth engine. Remote Sens Environ 2020;240(October 2018):111664. https://doi.org/10.1016/j.rse.2020.111664.
[7] Dieu PQ, Thao PTT. Urbanizing Mekong Delta in Vietnam: The challenges of urban expansion adapting to floods. In: The 5th International Conference of the International Forum on Urbanism (IFoU)–2011 the National University of Singapore, Department of Architecture–Global Visions: Risk and Opportunities for the Urban Planet; 2011.
[8] Donchyts G, Baart F, Winsemius H, Gorelick N, Kwadijk J, Van De Giesen N. Earth's surface water change over the past 30 years. Nature Climate Change 2016;6(9):810–3.
[9] Duc Tran D, Van Halsema G, Hellegers PJGJ, Phi Hoang L, Quang Tran T, Kummu M, et al. Assessing impacts of dike construction on the flood dynamics of the Mekong Delta. Hydrol Earth Syst Sci 2018;22(3):1875–96.
[10] Fisher RA. Statistical methods for research workers. In *breakthroughs in statistics*. Springer; 1992. p. 66–70.
[11] GFDRR. Toward integrated disaster risk Management in Vietnam. World Bank 2017. https://doi.org/10.1596/28871.
[12] Gorelick N, Hancher M, Dixon M, Ilyushchenko S, Thau D, Moore R. Google earth engine: planetary-scale geospatial analysis for everyone. Remote Sens Environ 2017;202:18–27.
[13] GSO. Statistical Yearbook of Vietnam 2020. Statistical Publishing House; 2021.
[14] Hansen MC, Potapov PV, Moore R, Hancher M, Turubanova SA, Tyukavina A, et al. High-resolution Global Maps. 2021.
[15] Hoang LP, Lauri H, Kummu M, Koponen J, Van Vliet MTH, Supit I, et al. Mekong River flow and hydrological extremes under climate change. Hydrol Earth Syst Sci 2016;20(7):3027–41.
[16] Johansen K, Phinn S, Taylor M. Mapping woody vegetation clearing in Queensland, Australia from Landsat imagery using the Google earth engine. Remote Sensing Appl Soc Environ 2015;1:36–49.
[17] Khan SI, Hong Y, Wang J, Yilmaz KK, Gourley JJ, Adler RF, et al. Satellite remote sensing and hydrologic modeling for flood inundation mapping in Lake victoria basin: implications for hydrologic prediction in ungauged basins. IEEE Trans Geosci Remote Sens 2011;49(1 PART 1):85–95. https://doi.org/10.1109/TGRS.2010.2057513.
[18] Kumar L, Mutanga O. Google earth engine applications since inception: usage, trends, and potential. Remote Sens (Basel) 2018;10(10):1–15. https://doi.org/10.3390/rs10101509.
[19] Lal P, Prakash A, Kumar A, Srivastava PK, Saikia P, Pandey AC, et al. Evaluating the 2018 extreme flood hazard events in Kerala, India. Remote Sensing Lett 2020;11(5):436–45.
[20] Landuyt L, Van Wesemael A, Schumann GJP, Hostache R, Verhoest NEC, Van Coillie FMB. Flood mapping based on synthetic aperture radar: an assessment of established approaches. IEEE Trans Geosci Remote Sens 2019;57(2):722–39. https://doi.org/10.1109/TGRS.2018.2860054.
[21] Le TA. Phân tích diễn biến lũ lụt và khô hạn ở Đồng bằng sông Cửu Long trong 20 năm gần đây. Vietnam J Sci Technol Eng 2020;62(11):22–7.
[22] Le TVH, Nguyen HN, Wolanski E, Tran TC, Haruyama S. The combined impact on the flooding in Vietnam's Mekong River delta of local man-made structures, sea level rise, and dams upstream in the river catchment. Estuar Coast Shelf Sci 2007;71(1–2):110–6.
[23] Loc HH, Van Binh D, Park E, Shrestha S, Dung TD, Son VH, et al. Intensifying saline water intrusion and drought in the Mekong Delta: from physical evidence to policy outlooks. Sci Total Environ 2021;757:143919.
[24] Long S, Fatoyinbo TE, Policelli F. Flood extent mapping for Namibia using change detection and thresholding with SAR. Environ Res Lett 2014;9(3):1–9. https://doi.org/10.1088/1748-9326/9/3/035002.
[25] MARD. Summary of the steering and management of responding drought, water shortage, saltwater intrusion, ensuring water sources for agricultural production. In: people in the Mekong Delta in the dry season 2019–2020. MARD (Ministry of Agriculture and Rural Development); 2020.
[26] Moharrami M, Javanbakht M, Attarchi S. Automatic flood detection using sentinel-1 images on the google earth engine. Environ Monit Assess 2021;193(5):1–17.
[27] Moothedan AJ, Dhote PR, Thakur PK, Garg V, Aggarwal SP, Mohapatra M. Automatic flood mapping using Sentinel-1 GRD SAR images and Google earth engine: A case study of Darbhangah, Bihar. In: The Proceedings of National Seminar on 'Recent Advances in Geospatial Technology and Applications; 2020.
[28] Mutanga O, Kumar L. Google earth engine applications. Remote Sens (Basel) 2019;11(5):11–4. https://doi.org/10.3390/rs11050591.
[29] Padarian J, Minasny B, McBratney AB. Using Google's cloud-based platform for digital soil mapping. Comput Geosci 2015;83:80–8. https://doi.org/10.1016/j.cageo.2015.06.023.
[30] Park E, Ho HL, Tran DD, Yang X, Alcantara E, Merino E, et al. Dramatic decrease of flood frequency in the Mekong Delta due to riverbed mining and dyke construction. Sci Total Environ 2020;723:138066.
[31] Patela NN, Angiuli E, Gamba P, Gaughan A, Lisini G, Stevens FR, et al. Multitemporal settlement and population mapping from landsatusing google earth engine. Int J Appl Earth Observ Geoinforma 2015;35(PB):199–208. https://doi.org/10.1016/j.jag.2014.09.005.

[32] PCBL. Report on the Socio-economic Situation in November and the First. 2020 [11 months of 2020].
[33] Pekel J-F, Cottam A, Gorelick N, Belward AS. High-resolution mapping of global surface water and its long-term changes. Nature 2016;540(7633):418–22.
[34] Pokhrel Y, Shin S, Lin Z, Yamazaki D, Qi J. Potential disruption of flood dynamics in the lower Mekong River basin due to upstream flow regulation. Sci Rep 2018;8 (1):1–13.
[35] Pramanick N, Acharyya R, Mukherjee S, Mukherjee S, Pal I, Mitra D, et al. SAR based flood risk analysis: a case study Kerala flood 2018. Adv Space Res 2021. https://doi.org/10.1016/j.asr.2021.07.003.
[36] Ratner B. The correlation coefficient: its values range between+ 1/− 1, or do they? J Target Measure Anal Market 2009;17(2):139–42.
[37] Singh G, Pandey A. Mapping Punjab flood using multi-temporal open-access synthetic aperture radar data in Google earth engine. In: Hydrological Extremes. Springer; 2021. p. 75–85.
[38] Tang Z, Li Y, Gu Y, Jiang W, Xue Y, Hu Q, et al. Assessing Nebraska playa wetland inundation status during 1985–2015 using Landsat data and Google earth engine. Environ Monit Assess 2016;188(12):1–14.
[39] Tay CWJ, Yun S-H, Chin ST, Bhardwaj A, Jung J, Hill EM. Rapid flood and damage mapping using synthetic aperture radar in response to typhoon Hagibis, Japan. Scientific Data 2020;7(1):1–9.
[40] Tiwari V, Kumar V, Matin MA, Thapa A, Ellenburg WL, Gupta N, et al. Flood inundation mapping-Kerala 2018; harnessing the power of SAR, automatic threshold detection method and Google earth engine. Plos One 2020;15(8): e0237324.
[41] Toan TQ. Climate change and sea level rise in the Mekong Delta: Flood, tidal inundation, salinity intrusion, and irrigation adaptation methods. In: Coastal disasters and climate change in Vietnam. Elsevier; 2014. p. 199–218.
[42] Tran DD, Dang MM, Du Duong B, Sea W, Vo TT. Livelihood vulnerability and adaptability of coastal communities to extreme drought and salinity intrusion in the Vietnamese Mekong Delta. Int J Disaster Risk Reduct 2021;57:102183. https://doi.org/10.1016/J.IJDRR.2021.102183.
[43] Trang PTH, Tuan TV. Flooding in the Mekong Delta: causes and solutions. J Sci Ho Chi Minh City Univ Educ 2016;3(158):158–69.
[44] Trang Pham Thi Huyen, Van Tuan T. Flooding in the Mekong Delta: causes and solutions. J Sci Ho Chi Minh City Univ Educ 2016;3(81):158–69.
[45] Triet NVK, Dung NV, Fujii H, Kummu M, Merz B, Apel H. Has dyke development in the Vietnamese Mekong Delta shifted flood hazard downstream? Hydrol Earth Syst Sci 2017;21(8):3991–4010.
[46] Twele A, Cao W, Plank S, Martinis S. Sentinel-1-based flood mapping: a fully automated processing chain. Int J Remote Sens 2016;37(13):2990–3004. https://doi.org/10.1080/01431161.2016.1192304.
[47] Van Binh D, Kantoush S, Sumi T. Changes to long-term discharge and sediment loads in the Vietnamese Mekong Delta caused by upstream dams. Geomorphology 2020;353:107011.
[48] Vanama VSK, Mandal D, Rao YS. GEE4FLOOD: rapid mapping of FLOOD areas using temporal Sentinel-1 SAR images with Google earth engine cloud platform. J Appl Remote Sens 2020;14(3):34505.
[49] Voigt S, Kemper T, Riedlinger T, Kiefl R, Scholte K, Mehl H. Satellite image analysis for disaster and crisis-management support. IEEE Trans Geosci Remote Sens 2007; 45(6):1520–8. https://doi.org/10.1109/TGRS.2007.895830.
[50] Xiong J, Thenkabail PS, Gumma MK, Teluguntla P, Poehnelt J, Congalton RG, et al. Automated cropland mapping of continental Africa using Google earth engine cloud computing. ISPRS J Photogr Remote Sens 2017;126:225–44. https://doi.org/10.1016/j.isprsjprs.2017.01.019.
[51] Pulvirenti L, Pierdicca N, Chini M, Guerriero L. An algorithm for operational flood mapping from Synthetic Aperture Radar (SAR) data using fuzzy logic. Natural Hazards and Earth System Sciences 2011;11(2):529–40.